Self-Assembled Monolayer of Light-Harvesting Core Complexes from Photosynthetic Bacteria on a Gold Electrode Modified with Alkanethiols

Masaharu Kondo, Yukari Nakamura, Kaoru Fujii, Morio Nagata, Yoshiharu Suemori, Takehisa Dewa, Kouji Iida,† Alastair T. Gardiner,‡ Richard J. Cogdell,‡ and Mamoru Nango*

Department of Applied Chemistry, Nagoya Institute of Technology, Gokiso-cho, Showa-ku, Nagoya 466-8555, Japan, Nagoya Municipal Industrial Research Institute, Rokuban 3-4-41, Atsuta-ku, Nagoya 456-0058, Japan, and Division of Biochemistry and Molecular Biology, Glasgow Biomedical Research Centre, Institute of Biomedical and Life Sciences, University of Glasgow, 126 University Place, G12 8TA, UK

Received March 30, 2007

Light-harvesting antenna core (LH1−RC) complexes isolated from *Rhodoseudomonas palustris* were self-assembled on a gold electrode modified with self-assembled monolayers (SAMs) of the alkanethiols $NH_2(CH_2)_nSH$, $n = 2$, 6, 8, 11; $HOOC(CH_2)_7SH$; and $CH_3(CH_2)_7SH$, respectively. Adsorption of the LH1−RC complexes on the SAMs depended on the terminating group of the alkanethiols, where the adsoption increased in the following order for the terminating groups: amino groups > carboxylic acid groups > methyl groups. Further, the adsorption on a gold electrode modified with SAMs of $NH_2(CH_2)_nSH$, $n = 2$, 6, 8, 11, depended on the methylene chain length, where the adsorption increased with increasing the methylene chain length. The presence of the well-known light-harvesting and reaction center peaks of the near infrared (NIR) absorption spectra of the LH1−RC complexes indicated that these complexes were only fully stable on the SAM gold electrodes modified with the amino group. In the case of modification with the carboxyl group, the complexes were partially stable, while in the presence of the terminal methyl group the complexes were extensively denatured. An efficient photocurrent response of these complexes on the SAMs of $NH_2(CH_2)_nSH$, $n = 2$, 6, 8, 11, was observed upon illumination at 880 nm. The photocurrent depended on the methylene chain length (n), where the maximum photocurrent response was observed at $n = 6$, which corresponds to a distance between the amino terminal group in $NH_2(CH_2)_6SH$ and the gold surface of 1.0 nm.

Introduction

When light energy is absorbed in vivo by purple bacterial light-harvesting (LH) complexes, it is rapidly transferred to the reaction centers (RC) where light energy is efficiently converted into useful chemical energy.[1] In most types of purple bacteria, there are two types of antenna complexes: peripheral LH2 complexes and the LH1 complexes.[1] The structure of the LH2 complex of *Rhodopseudomonas acidophila* strain 10050 has been resolved to a resolution of 2.0 Å.[2] This LH2 complex consists of a ring of nine heterodimeric subunits. However, such a high-resolution structure has not yet been determined for the LH1 complex. There are low-resolution projection structures produced by transmission electron microscopy (TEM) of two-dimensional (2D) crystals of the LH1 complex and a 4.8 Å X-ray crystal structure of the LH1−RC core complex.[3−5] The recent crystal structure of the LH1−RC "core" complex from *Rhodoseudomonas palustris* reveals that the LH1 complex surrounds the contours of the RC so that the core complex has an overall oval rather than circular shape.[4] This structure shows that the RC is surrounded by the LH1 complex, which consists of 15 pairs of transmembrane helical α- and β-polypeptides and their coordinated bacteriochlorophylls (BChls). Atomic force microscopy (AFM) has also been used to observe antenna complexes in both natural and reconstituted membranes.[6−12]

Organic compounds and devices whose design has been inspired by photosynthesis are being extensively studied in the field of interfacial science. Imahori et al. assembled organic compounds such as porphyrins and fullerenes onto a gold electrode or gold colloids as photoconversion devices and catalysts.[13,14] Amao et al. adsorbed chlorophyll derivatives on TiO_2 substrates to construct photoelectron conversion devices and hydrogen evolution systems.[15,16] Okura et al. demonstrated that photosystem I with cytochrome c_3 cross-linked to [NiFe]-hydrogenase is capable of hydrogen evolution.[17] Dutton et al., Miyake et al., and Cotton et al. have all reported on devices using LB films containing bacterial RCs.[18−20] Trammell et al. reported orientated binding of RC on a gold electrode by a polyhistidine tag method.[21]

Our current understanding of energy transfer and charge separation reactions in the LH2 and LH1−RC complexes has enabled the first step to be taken toward generating from them artificial systems that convert light energy into usable electrical current. Previous attempts to produce an artificial, energy-converting electrode system used either the LH1 complexes[22] or RC[23] immobilized on the electrodes. Until now, however, there have only been a few attempts to immobilize intact core complexes consisting of both the LH1 complex and the RC components together onto an electrode.[24,25] We have recently developed a procedure to create a self-assembled monolayer

* Corresponding author. Fax & Tel: +81-52-735-5226. E-mail: nango@nitech.ac.jp.
† Nagoya Municipal Industrial Research Institute.
‡ University of Glasgow.

10.1021/bm070352z CCC: $37.00
Published on Web 06/26/2007

(SAM) of reconstituted LH1 complexes on a transparent indium tin oxide (ITO) electrode modified with aminopropylsilane (APS) between the electrode surface and the anionic LH1 polypeptides at pH 8.0.[22] The NIR absorption spectrum showed that the LH1 complex was stable when immobilized onto these electrodes. This study was extended using native LH1−RC complexes. LH1−RC complexes isolated from *Rhodospirillum rubrum* and *R. palustris* were successfully assembled on an ITO electrode modified with APS (APS-ITO).[24] Efficient energy transfer and photocurrent responses could be observed upon illumination at 880 nm.

The object of this present work is to explore the use of SAM molecules for adsorbing LH1−RC complexes from *R. palustris* onto gold electrodes and how these complexes affect the efficiency of electron transfer between these complexes and the electrode. This is the first report to attempt the assembly of the LH1−RC complex on a gold electrode, although the report of RC is well developed. In this area of research there are two fundamental issues: first, how to order proteins on the electrodes with respect to their sidedness, and second, how to make a good electrical contact between the protein and the electrode. The adsorption of functional membrane proteins onto substrates is very difficult, because they often denature and their inherent electron-transfer capability is then compromised. Chemical modification of the gold electrodes is commonly used to solve this problem. In addition, these chemical modifications also play a critical role in making a good electric contact between membrane protein and gold electrode.[25−30]

However, there are rather few reports of studies looking for better chemical modifiers of gold electrodes for membrane proteins. In this study, we have tested alkanethiols terminating in amino [$NH_2(CH_2)_6SH$, 6-amino-1-hexanethiol, 6-AHT], carboxylic acid [$HOOC(CH_2)_7SH$, 7-carboxy-1-heptanethiol, 7-CHT], and methyl [$CH_3(CH_2)_7SH$, 1-octanethiol, OCT] groups. The effect of changes in chain length of $NH_2(CH_2)_nSH$ ($n = 2$, 6, 8, 11) on the ability of the gold electrode to adsorb the LH1−RC complexes and on their subsequent photocurrent activity was also investigated with the aim of using this core complex in a nanodevice.

Materials and Methods

Growth of *R. palustris*. The photosynthetic bacteria *R. palustris* were grown anaerobically in the light in modified Hutner's media as previously described.[4,31]

Isolation and Purification of the LH1−RC Complex. The LH1−RC complexes, isolated from *R. palustris*, were purified essentially as described previously.[4] The photosynthetic membranes were solubilized by the addition of 1% LDAO (v/v) in 20 mM Tris HCl pH 8.0. The LH1−RC complex was then separated from the LH2 complexes by sucrose density centrifugation at 225 000*g* for 16 h at 4 °C, using an Hitachi CP 70M with P45AT rotor. The LH1−RC complex was further purified by DE52 anion-exchange chromatography. LH1−RC complexes with a purity ratio of $OD_{880}/OD_{280} > 2.2$ were used for assembly onto the gold electrodes.

Preparation of the LH1−RC Complex Assembled on Gold Electrodes. Electrodes were prepared by evaporation of 20 nm Au onto a 5 nm Ti layer on a clean glass plate (2 cm^2). The gold electrodes were incubated in chloroform solutions of the alkanethiols, containing 10 mM $NH_2(CH_2)_6SH$ (6-amino-1-hexanethiol, 6-AHT), 10 mM $HOOC(CH_2)_7SH$ (7-carboxy-1-heptanethiol, 7-CHT), or 10 mM $CH_3(CH_2)_7SH$ (1-octanethiol, OCT) for 12 h at 25 °C. The electrodes were then carefully rinsed with chloroform and blown dry with nitrogen. After formation of the alkanethiol monolayers, the electrodes were again incubated in a 20 mM Tris-HCl solution (pH 8.0) containing the LH1−RC complex at an OD of 1.0 cm^{-1} at 880 nm.

NIR Absorption Spectroscopy. NIR absorption spectra were recorded with Hitachi U-2000 and U-3500 spectrophotometers. The electrodes, covered by LH1−RC complexes, were placed perpendicular to the light beam in a quartz cuvette. A reference baseline was recorded with the gold electrode without LH1−RC complexes.

Cyclic Voltammetry. CV data were recorded with a Hokuto Denko HZ-3000 potentiostat; Ag/AgCl (0.1 M KCl) served as the reference electrode, and platinum was the counter electrode. The measurements were done in 0.1 M phosphate buffer (pH 7.0), containing 1 mM $K_3[Fe(CN)_4]$, and 0.1 M $NaClO_4$ as the supporting electrolyte. All solutions were degassed by nitrogen bubbling.

Photocurrent Measurements. Photocurrents were measured at −0.2 V vs Ag/AgCl in a home-made cell (100 cm^3) that contained three electrodes: a gold electrode incorporating the LH1−RC complex as a working electrode, an Ag/AgCl (saturated KCl) as a reference electrode, and a platinum flake as a counter electrode. The working electrode was illuminated with a xenon lamp unit (SM-25, Bunkokeiki, Japan), through a monochromator. The solution consisted of 0.1 M phosphate buffer (pH 7.0), containing 0.1 M $NaClO_4$ and 5 mM methyl viologen as an electron acceptor.

Results and Discussion

Figure 1 shows a model of the self-assembly of LH1−RC complexes onto a gold electrode modified with alkanethiol SAMs, together with a possible electron-transfer pathway from the electrode to the RC. The H-chain is oriented toward the aqueous phase (Up), while it is oriented toward the electrode (Down). The electron-transfer pathway in the RC is unidirectional from the BChl dimer (SP), to the monomeric BChl *a*, to the bacteriopheophytin (Bpho), and finally to the quinone (Q) (H-chain) as shown in Figure 1b. Methyl viologen is used as an electron acceptor. This photoinduced electron-transfer system will only work if the LH1−RC complex is correctly oriented as shown in this figure.

Redox Properties of Ferricyanide Using Gold Electrodes Modified with SAMs. Figure 2 shows the CV of ferricyanide using a gold electrode modified with 6-AHT, 7-CHT, and OCT. Similar redox potentials and conductivity for ferricyanide were observed for 6-AHT and OCT as well as for bare electrodes, although with OCT the level of conductivity was reduced. No redox peaks for ferricyanide were observed when the electrodes were modified with 7-CHT, implying that the anionic surface on the gold electrode inhibits the interaction with ferricyanide.[32]

Figure 3 shows the CV for ferricyanide using a gold electrode modified with SAMs of $NH_2(CH_2)_nSH$ ($n = 2$, 6, 8, 11). The measured electrochemical properties of ferricyanide depended on the methylene chain length. Good conductivity for ferricyanide was observed with electrodes modified with 2-AET and 6-AHT as well as for bare electrode. The conductivity for ferricyanide was attenuated in the presence of 8-AOT and 11-AUT. These results suggest that the SAM materials modified with $NH_2(CH_2)_nSH$ such as for 8-AOT and 11-AUT are sufficiently densely packed onto the gold electrode to inhibit electron transfer between the electrode and ferricyanide. The redox response of ferricyanide was clearly observed for electrodes modified with 2-AET and 6-AHT, as well as for a bare electrode. Again in the case of modification with 8-AOT and 11-AUT the CV response of ferricyanide was suppressed. The conductivity of electrode decreased with increasing the methylene chain length of SAM. It has been reported that in general as the length of a long chain alkanethiol SAM increases it becomes more densely packed and so the blocking of Au surface also increases.[33] In this study, the long chain alkanethiol SAMs, such 8-AOT and 11-AUT, are likely to be densely

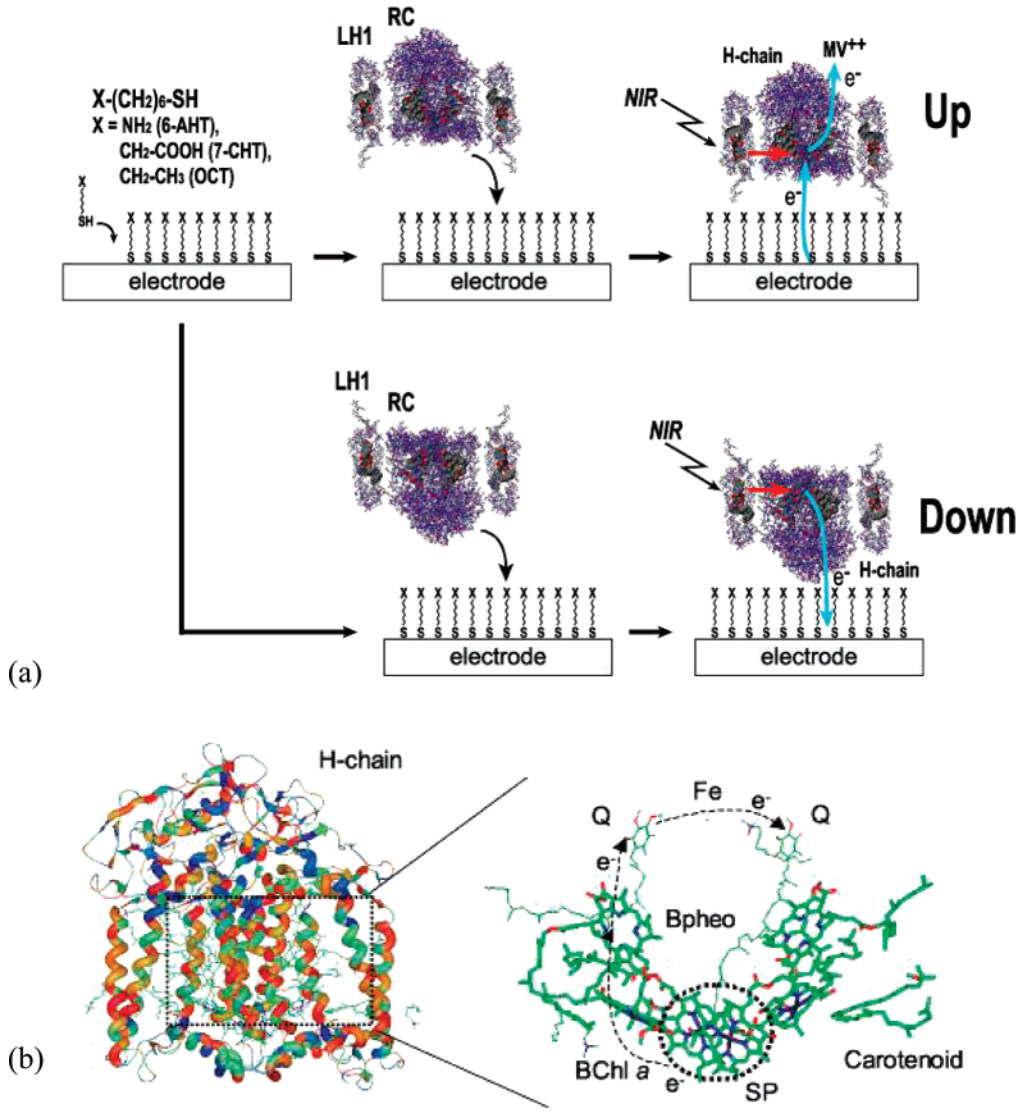

Figure 1. Schematic model of assembly of LH1−RC complex on the electrode modified with alkanethiols (a) and electron-transfer pathway of RC (b). (a) The C-terminus of the LH1 complex and the SP side of RC is oriented toward hydrophilic SAMs on the gold substrate and the H-chain is oriented toward the aqueous phase (Up), while the H-chain is oriented toward the electrode (Down). (b) Electrons are transferred along the pigments associated with the L-chain of the RC, i.e., from SP to BChl *a* (0.47 nm transfer distance), to Bpheo (0.38 nm transfer distance), and finally to Q (0.9 nm transfer distance).

packed on the gold electrode and so inhibit electron transfer between the gold electrode and the ferricyanide. Where this electron transfer does depend on tunneling the rate of this transfer should decrease exponentially as a function of the distance between the ferricyanide and the surface of electrode. Porter et al. noted that the distance between the end of the SAM and electrode was 1.0, 1.4, and 2.1 nm, respectively, when n = 6, 8, and 11 for the alkyl compound.[33] This conductivity data as a function of the type of SAM is important, since it will affect the size of the photocurrent responses described below.

NIR Absorption Spectra of the LH1−RC Complexes on SAM-Modified Gold Electrodes. Figure 4 shows NIR absorption spectra of the LH1−RC complexes in aqueous solution and on a gold electrode modified with 6-AHT, 7-CHT, and OCT. The amount of adsorption of the LH1−RC complexes was 6-AHT > 7-CHT > OCT. This spectrum indicates that the LH1−RC complexes assembled on 6-AHT and 7-CHT SAM-modified gold electrodes are native, since they have an absorption maximum at 880 nm with a smaller peak at 800 nm, consistent with the spectrum of the complex in aqueous solution.

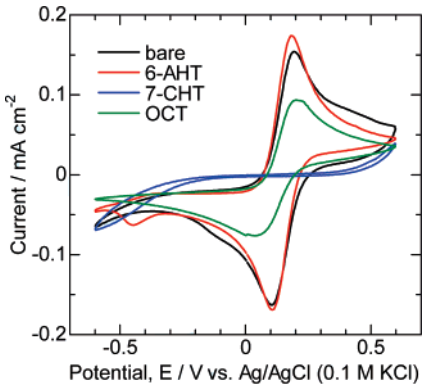

Figure 2. Cyclic voltammograms of ferricyanide for 6-amino-1-hexanethiol (6-AHT) (red), 7-carboxyl-1-heptanethiol (7-CHT) (blue), and 1-octanethiol (OCT) (green) self-assembled onto a gold electrode and a bare gold electrode (black) in 0.1 M phosphate buffer containing 1 mM $K_3[Fe(CN)_6]$ and 0.1 M $NaClO_4$. The scan rate was 0.1 V s^{-1}.

Similar results were observed with $NH_2(CH_2)_nSH$, n = 2, 8, 11. In the case of OCT, the complexes are not absorbed. Figure

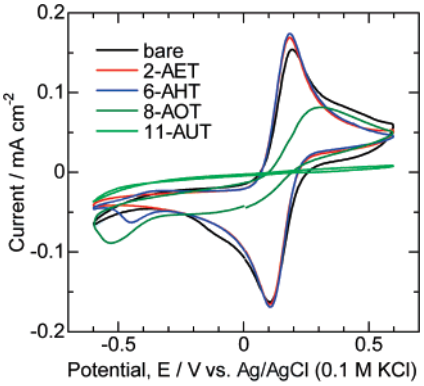

Figure 3. Cyclic voltammograms of ferricyanide for $NH_2(CH_2)_nSH$, n = 2 (2-amino-1-ethanethiol, 2-AET) (red), n = 6 (6-amino-1-hexanethiol, 6-AHT) (blue), n = 8 (8-amino-1-octanethiol, 8-AOT) (green), n = 11 (11-amino-1-undecanthiol, 11-AUT) (light green) self-assembled onto a gold electrode and a bare gold electrode (black) in 0.1 M phosphate buffer containing 1 mM $K_3[Fe(CN)_6]$ and 0.1 M $NaClO_4$. The scan rate was 0.1 V s^{-1}.

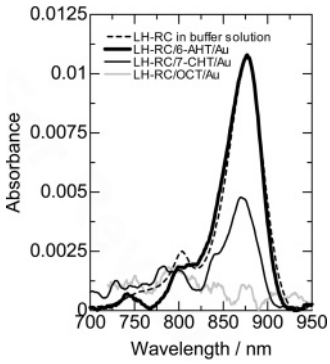

Figure 4. NIR absorption spectra of LH1−RC complex in 20 mM Tris-HCl buffer (pH 8.0) (broken line) and adsorbed on a gold electrode modified with 6-amino-1-hexanethiol (6-AHT) (bold line), 7-carboxyl-1-heptanethiol (7-CHT) (solid line), and 1-octanethiol (OCT) (gray line).

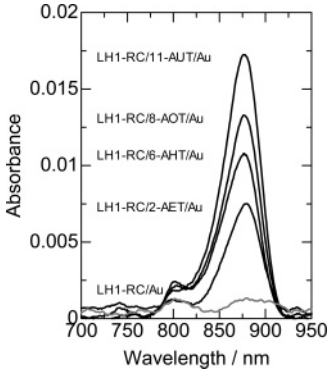

Figure 5. NIR absorption spectra of LH1−RC complex adsorbed on a gold electrode modified with $NH_2(CH_2)_nSH$, n = 2 (2-amino-1-ethanethiol, 2-AET), n = 6 (6-amino-1-hexanethiol, 6-AHT), n = 8 (8-amino-1-octanethiol, 8-AOT), n = 11 (11-amino-1-undecanthiol, 11-AUT), and a bare gold electrode (gray line).

5 shows the absorption spectra of LH1−RC complexes assembled on a gold electrode modified with $NH_2(CH_2)_nSH$, n = 2 (2-AET), n = 6 (6-AHT), n = 8 (8-AOT), and n = 11 (11-AUT), respectively. The amount of adsorption of LH1−RC complex increased with increasing methylene chain length. This effect is shown in detail in Figure 6.

Photoinduced Electron Transfer from the LH1−RC Complexes on SAM-Modified Electrodes. Figure 7 shows the photocurrent response of the LH1−RC complexes on gold

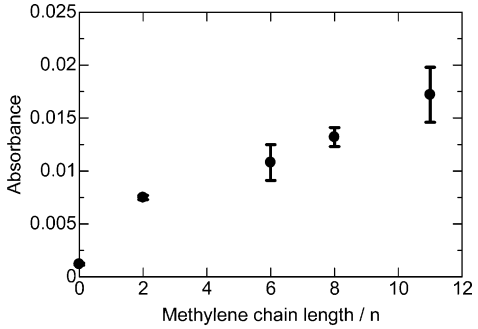

Figure 6. Plots of absorbance of LH1−RC complex adsorbed on a gold electrode modified with $NH_2(CH_2)_nSH$, n = 2 (2-amino-1-ethanethiol, 2-AET), n = 6 (6-amino-1-hexanethiol, 6-AHT), n = 8 (8-amino-1-octanethiol, 8-AOT), and n = 11 (11-amino-1-undecanthiol, 11-AUT), and bare gold electrode (n = 0).

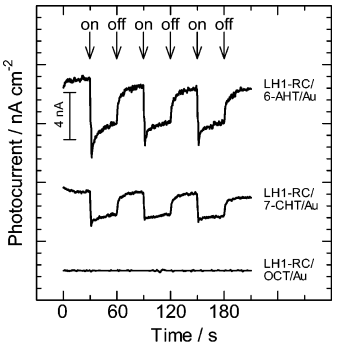

Figure 7. Photocurrent response of LH1−RC complex assembled on a gold electrode modified with 6-amino-1-hexanethiol (6-AHT), 7-carboxyl-1-heptanethiol (7-CHT), and 1-octanethiol (OCT) in buffer solution when illuminated at 880 nm.

Table 1. Absorbance of the Near-IR Absorption at 880 nm, Photocurrent Density (Normalized for Absorbance at 880 nm), and Quantum Yield

SAM	absorbance	photocurrent density ($\times 10^7$ A cm^{-2} Abs^{-1})	quantum yield[a] ($\times 10^3$%)
2-AET	0.0075	1.8 ± 0.3	3.2 ± 0.4
6-AHT	0.0108	5.1 ± 0.5	8.7 ± 0.8
8-AOT	0.0133	1.7 ± 0.1	3.0 ± 0.1
11-AUT	0.0172	0.8 ± 0.3	1.3 ± 0.5
7-CHT	0.0046	4.3	7.5
OCT	0.0018	0.0	0.0

[a] $\phi = (il e)/[I(1 - 10^{-A})]$, $I = (W\lambda)/(hc)$, where i is the photocurrent density, e is the elementary charge, I is number of photons per unit area and unit time, A is absorbance of the adsorbed LH1−RC complex at λ (nm), λ is the wavelength of light irradiation, W is light power irradiated at λ (nm), c is the light velocity, and h is the Planck constant.

electrodes modified with 6-AHT, 7-CHT, and OCT, when these electrodes are illuminated with pulsed light at 880 nm. Cathodic photocurrents were observed, indicating that one-way electron transfer from pigments in the core complex to methyl viologen occurred.[34,35] Furthermore, the photocurrent density, normalized for the amount of LH1−RC complex adsorbed, was in the following order: 6-AHT > 7-CHT ≫ OCT (Table 1). The photocurrent was, therefore, sensitive to the surface properties of the SAMs on the gold electrode.

Figure 8 shows the action spectrum of the photocurrent and NIR absorption spectrum for the LH1−RC complexes assembled onto a 6-AHT-modified gold electrode. The photocurrent response was wavelength dependent and showed a maximum at the wavelength corresponding to the maximum absorption

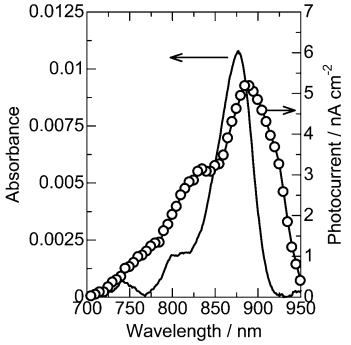

Figure 8. NIR absorption and action spectra of LH1−RC complex assembled on a gold electrode modified with 6-amino-1-hexanethiol (6-AHT).

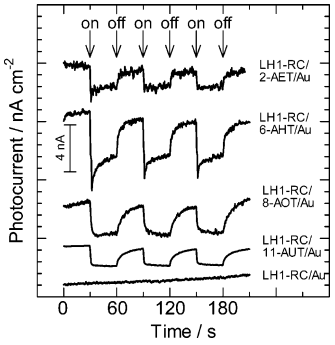

Figure 9. Photocurrent response of LH1−RC complex assembled on a gold electrode modified with 2-amino-1-ethanethiol (2-AET), 6-amino-1-hexanethiol (6-AHT), 8-amino-1-octanethiol (8-AOT), and 11-amino-1-undecanthiol (11-AUT) and a bare gold electrode in buffer solution when illuminated at 880 nm.

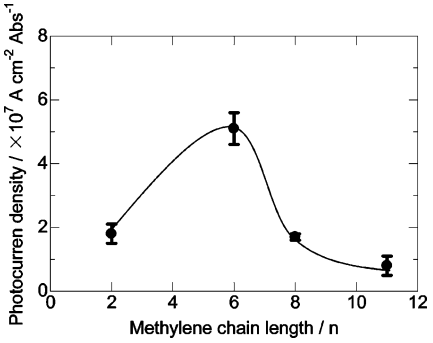

Figure 10. Plots of photocurrent density (A cm^{-2} Abs^{-1}) of LH1−RC complex assembled on a gold electrode modified with $NH_2(CH_2)_n$SH, n = 2 (2-amino-1-ethanethiol, 2-AET), n = 6 (6-amino-1-hexanethiol, 6-AHT), n = 8 (8-amino-1-octanethiol, 8-AOT), and n = 11 (11-amino-1-undecanthiol, 11-AUT).

band of the complexes. The quantum yield using 6-AHT was 8.7×10^{-3}% (Table 1).[35]

Figure 9 shows the photocurrent response of the LH1−RC complexes on a gold electrode modified with $NH_2(CH_2)_n$SH (n = 2, 6, 8, 11) when illuminated with pulsed light at 880 nm. The photocurrent depended on the methylene chain length of the SAM. Figure 10 shows that the plot of photocurrent density vs methylene chain length shows a maximum at n = 6. All of this data is summarized in Table 1. Interestingly, the photocurrent using 2-AET was lower than that using 6-AHT, possibly suggesting that if the gold electrode is too close to the LH1−RC complex it is able to quench the excited singlet states in the LH1. Such an effect has been reported by Imahori et al. with SAM-linked porphyrins on a gold electrode.[35,36] When the chain length of the SAM was short, below 0.6 nm, the excited singlet porphyrin was quenched by a gold electrode by direct energy transfer to the gold. Beyond n = 6, the photocurrent became lower with increasing methylene chain length. This probably reflectes the increased insulation effect of the longer SAMs (see Figure 3). Thus, the rate-determining step of the electron transfer is probably between the electrode and the LH1−RC complex. Since this electron transfer occurs by tunneling, the electron-transfer rates should decrease exponentially as a function of the distance between the pigment in RC and the surface of electrode. The distance between the amino terminal group in $NH_2(CH_2)_6$SH and the Au surface can be calculated to be 1.0 nm.[33] Direct electron transfer from electrode to methyl viologen can be simply ruled out due to the excessively large tunneling distances that would be required to traverse the protein, e.g., 7.3 nm across the RC.[37] Also the applied voltage was too low to induce electron transfer to methyl viologen (−0.62 V vs Ag/AgCl). Since the X-ray crystal structure of the RC has been described, this information can be used to propose the pathway of the multistep electron-transfer catalyzed by RC from the electrode to methyl viologen.

In Figure 1 the 3D structure of the RC is shown and the electron-transfer pathway derived from spectroscopic experiments.[38] Direct excitation with light or, indirectly, by resonance energy transfer from an antenna complex first promotes an electron from SP to an excited singlet state. Electrons are then transferred along the pigments associated with the L-chain of the RC, i.e., from SP to BChl *a* (0.47 nm transfer distance), to Bpheo (0.38 nm transfer distance), and finally to Q (0.9 nm transfer distance). In this study, it is not clear where the link to MV takes place; it could be via BChl or Bpheo, since the redox potential of MV is much lower than that of Q in the RC. The oxidized SP is then reduced by electron transfer from the gold electrode. The distance from SP to the surface of RC is likely to be 1.0 nm.[39] It is important, therefore, for this model to immobilize the LH1−RC complex on various substrates with a defined orientation relative to the electrode, as shown in Figure 1a (Up).

Adsorption of the LH1−RC complexes on the SAMs depended on the terminating group of alkanethiols, where the adsorption increased in the following order for the terminating group: amino group (6-AHT) > carboxylic acid group (7-CHT) > methyl group (OCT). Further, the adsorption of the LH1−RC complexes on a gold electrode modified with SAMs of $NH_2(CH_2)_n$SH, n = 2, 6, 8, 11, depended on the methylene chain length, where the adsorption increased with increasing the methylene chain length. However, in the case of SAMs with 2-AET, 8-AOT, and 11-AUT, the adsorbed complexes did not show efficient photocurrents and quantum yields. The maximum photocurrent response was observed at n = 6 among these compounds. It is important, therefore, when suitable materials for use as SAM compounds are considered, that not only the surface property of the terminating groups of the SAM are tested but also the methylene chain length.

Fotiadis et al. have discovered using AFM that the H-chain of the LH1−RC complex protrudes from the cytoplasmic membrane (by 4 nm),[9] consistent with our AFM images, which suggests that the SP side of LH1−RC complexes contact the mica (see the Supporting Information). This suggests that the C-terminus of LH1 is preferentially more adsorbed on the mica rather than the H-chain of RC (Figure 1). The C-terminus of the LH1-α and β polypeptides of the *R. palustris* LH1−RC complexes contain many polar amino acids. These are likely to be the reason why the C-terminus of the LH1 complex and the SP side of RC were preferentially adsorbed on the gold electrode

modified with 6-AHT by electrostatic interactions or hydrogen bonding between the SAM surface and LH1 polypeptides and why the H-chain was preferentially oriented toward the aqueous phase (see, Figure 1, Up). Since the photocurrent density was clearly dependent on the methylene chain length, this suggests that the rate-determining step of the photoinduced electron transfer might be between SP and the electrodes. This may explain why our results suggest that the C-terminus of LH1 complex and the SP side of RC were preferentially oriented onto the hydrophilic mica and why the H-chain was preferentially oriented toward the aqueous phase. A gold electrode modified with amino-terminated SAMs provided a hydrophilic surface as well as the mica. Therefore, the LH1−RC complexes may be oriented toward the aqueous phase (see Figure 1, Up).

For either LH1 complexes or the RC alone on an ITO electrode modified with APS very little, if any, photocurrent was observed.[40] When the LH1 complex of *Rh. rubrum* alone was immobilized on the electrode, the observed photocurrent was mainly generated by light absorbed at 770 nm, i.e., from monomeric BChl *a*.[34] The present data, taken together with these previous studies, indicates that the LH1−RC complex of *R. palustris* was rather stable and well-organized on the electrode, and the photocurrents were driven by light that was initially absorbed by the LH components. If the direction of LH1−RC complex is not well-organized, the photocurrent was not observed, because the distance between SP and the gold surface is too far. The LH1−RC complexes on the SAMs are, therefore, useful for studying electron transfer from electrodes to the complex as well as for applications in energy transfer devices and nonlinear optics.[21,25]

Conclusions

LH1−RC complexes isolated from *R. palustris* were successfully self-assembled on a gold electrode modified with SAMs of alkanethiols. The SAM method is clearly successful in assembling functional LH1−RC core complexes on the surface of gold electrode. Adsorption of the LH1−RC complexes on the SAMs depended on the chemical nature of the terminating group of the alkanethiols, where the adsorption increased in the following order: amino group > carboxylic acid group > methyl group. Further, the adsorption on a gold electrode modified with SAMs of $NH_2(CH_2)_nSH$, $n = 2$, 6, 8, 11, showed a strong dependence on the length of the methylene chain. The methylene chain length not only plays an important role for the assembly but also in the control of the electron-transfer efficiency, where the maximum photocurrent response was observed at $n = 6$. These results provide useful information about the effect of surface modification of electrodes on the performance of LH1−RC complexes as solar energy converters and on their stability.

Acknowledgment. M.N. is grateful to the international joint grant of JST and BBSRC for financial support. The present work was partially supported by a Grant-in-Aid for Scientific Research from the Ministry of Education, Culture, Sports, Science and Technology (MEXT) of Japanese Government and AOARD-06-4084.

Supporting Information Available. AFM procedures and AFM image of LH1−RC complexes from *R. palustris* on mica. This material is available free of charge via the Internet at http://pubs.acs.org.

References and Notes

(1) Ke, B. *Photosynthesis*; Govindjee, Ed.; Kluwer Academic Publishers: Norwell, MA, 2001.
(2) McDermott, G.; Prince, S. M.; Freer, A. A.; Hawthornthwaite-Lawless, A. M.; Papiz, M. Z.; Cogdell, R. J.; Isaacs, N. W. *Nature* **1995**, *374*, 517−521.
(3) Karrasch, S.; Bullough, P.; Ghosh, R. *EMBO J.* **1995**, *14*, 631−638.
(4) Roszak, A. W.; Howard, T. D.; Southall, J.; Gardiner, A. T; Law, C. J.; Isaacs, N. W.; Cogdell, R. J. *Science* **2003**, *302*, 1969−1972.
(5) Jungas, C.; Ranck, J.-L; Rigaud, J.-L.; Joliot, P.; Verméglio, A. *EMBO J.* **1999**, *18*, 534−542.
(6) Scheuring, S.; Reiss-Husson, F.; Engel, A.; Rigaud, J.-L.; Ranck, J.-L. *EMBO J.* **2001**, *20*, 3029−3035.
(7) Scheuring, S.; Seguin, J.; Marco, S.; Levy, D.; Robert, B.; Rigaud, J.-L. *Proc. Natl. Acad. Sci. U.S.A.* **2003**, *100*, 1690−1693.
(8) Scheuring, S.; Sturgis, J. N.; Prima, V.; Bernadac, A.; Lèvy, D.; Rigaud, J.-L. *Proc. Natl. Acad. Sci. U.S.A.* **2004**, *101*, 11293−11297.
(9) Fotiadis, D.; Qian, P.; Philippsen, A.; Bullough, P. A.; Engel, A.; Hunter, C. N. *J. Biol. Chem.* **2004**, *279*, 2063−2068.
(10) Bahatyrova, S.; Frese, R. N.; van der Werf, K. O.; Otto, C.; Hunter, C. N.; Olsen J. D. *J. Biol. Chem.* **2004**, *279*, 21327−21333.
(11) Bahatyrova, S.; Frese, R. N.; Siebert, C. A.; Olsen, J. D.; van der Werf, K. O.; van Grondelle, R; Niederman, R. A.; Bullough, P. A.; Otto, C.; Hunter, C. N. *Nature* **2004**, *430*, 1058−1062.
(12) Stamouli, A.; Kafi, S.; Klein, D. C. G.; Oosterkamp, T. H.; Frenken, J. W. M.; Cogdell, R. J.; Aartsma, T. J. *Biophys. J.* **2003**, *84*, 2483−2491.
(13) Imahori, H.; Norieda, H; Ozawa, S.; Ushida, K.; Yamada, H.; Azuma, T.; Tamaki, K.; Sakata, Y. *Langmuir* **1998**, *14*, 5335−5338.
(14) Imahori, H.; Kashiwagi, Y.; Endo, Y.; Hanada, T.; Nishimura, Y.; Yamazaki, I.; Araki, Y.; Ito, O.; Fukuzumi, S. *Langmuir* **2004**, *20*, 73−81.
(15) Aoki, K.; Takeuchi, Y.; Amao, Y. *Bull. Chem. Soc. Jpn.* **2005**, *78*, 132−134.
(16) Saiki, Y.; Amao, Y. *Bioconjugate Chem.* **2002**, *13*, 898−901.
(17) Ihara, M.; Nishihara, H.; Yoon, K. S.; Lenz, O.; Friedrich, B.; Nakamoto, H.; Kojima, K.; Honma, D.; Kamachi, T.; Okura, I. *Photochem. Photobiol.* **2006**, *82*, 676−682.
(18) Alegria, G.; Dutton, P. L. *Biochem. Biophys. Acta* **1991**, *1057*, 239−257.
(19) Yasuda, Y.; Hirata, Y; Sugino, H.; Kumei, M.; Hara, M.; Miyake, J.; M. Fujihira, M. *Thin Solid Films* **1992**, *210−211*, 733−735.
(20) Fang, J. Y.; Gaul, D. F.; Chumanov, G.; Cotton, T. M.; Uphaus, R. A. *Langmuir* **1995**, *11*, 4366−4370.
(21) Trammell, S. A.; Wang, L.; Zullo, J. M.; Shashidhar, R.; Lebedev, N. *Biosens. Bioelectron.* **2004**, *19*, 1649−1655.
(22) Ogawa, M.; Kanda, R.; Dewa, T.; Iida, K.; Nango, M. *Chem. Lett.* **2002**, *31*, 466−467.
(23) Blankenship, R. E.; Madigan, M. T.; Bauer, C. E. *Anoxygenic Photosynthetic Bacteria*; Kluwer Academic Pubrishers: Dorderecht, 1995.
(24) Ogawa, M.; Shinohara, K.; Nakamura, Y.; Suemori, Y.; Nagata, M.; Iida, K.; Gardiner, A. T.; Cogdell, R. J.; Nango, M. *Chem. Lett.* **2004**, *33*, 772−773.
(25) Das, R.; Kiley, P. J.; Segal, M.; Norville, J.; Yu, A. A.; Wang, L.; Trammell, S. A.; Reddick, L. E.; Kumar, R.; Stellacci, F.; Lebedev, N.; Schnur, J.; Bruce, B. D.; Zhang, S.; Baldo, M. *Nano Lett.* **2004**, *4*, 1079−1083.
(26) Sagara, T.; Niwa, K.; Sone, A.; Hinnen, C.; Niki, K. *Langmuir* **1990**, *6*, 254−262.
(27) Taniguchi. I.; Ishimoto, H.; Miyagawa, K.; Iwai, M.; Nagai, H.; Hanazono, H.; Taira, K.; Kubo, A.; Nishikawa, A.; Nishiyama, K.; Dursun, Z.; Hareau, G. P.-J.; Tazaki, M. *Electrochem. Commun.* **2003**, *5*, 857−861.
(28) Mikayama, T.; Miyashita, T.; Iida, K.; Suemori, Y.; Nango, M. *Mol. Cryst. Liq. Cryst.* **2006**, *445*, 291−296.
(29) Matsumoto, K.; Nomura, K.; Tohnai, Y.; Fujioka, S.; Wada, M.; Erabi, T. *Bull. Chem. Soc. Jpn.* **1999**, *72*, 2169−2175.
(30) Crittenden, S. R.; Sund, C. J.; Summer, J. J. *Langmuir* **2006**, *22*, 9473−9476.
(31) Visschers, R. W.; Chang, M. C.; van Mourik, F.; Parkes-Loach, P. S.; Heller, B. A.; Loach, P. A.; van Grondelle, R. *Biochemistry* **1991**, *30*, 5734−5742.
(32) Takehara, K.; Takemura, H.; Ide, Y. *Electrochim. Acta* **1994**, *39*, 817−822.
(33) Poter, M. D.; Bright, T. B.; Allara, D. L.; Chidsey, C. E. D. *J. Am. Chem. Soc.* **1987**, *109*, 3559−3568.
(34) Nagata, M.; Yoshimura, Y.; Inagaki, J.; Suemori, Y.; Iida, K.; Ohtsuka, T.; Nango, M. *Chem. Lett.* **2003**, 852−853.
(35) Imahori, H.; Yamada, H.; Nishimura, Y.; Yamazaki, I.; Sakata, Y. *J. Phys. Chem. B* **2000**, *104*, 2099−2108.

(36) Imahori, H.; Norieda, H.; Nishimura, Y.; Yamazaki, I.; Higuchi, K.; Kato, N.; Motohiro, T.; Yamada, H.; Tamaki, K.; Arimura, M.; Sakata, Y. *J. Phys. Chem. B* **2000**, *104*, 1253−1260.
(37) Pomerantz, M.; Aviram, M. R. A.; Li, L.; Schrott, A. G. *Science* **1992**, *255*, 1115−1158.
(38) Feher, G.; Allen, J. P.; Okamura, M. Y.; Rees, D. C. *Nature* **1989**, *339*, 111−116.
(39) The distance from SP of RC to the interface of RC protein, Y162 (L-subunit of RC), is calculated from PDB (Protein Data Bank) ID 1AIJ.
(40) Suemori, Y.; Fujii, K.; Ogawa, M.; Nakamura, Y.; Shinohara, K.; Nakagawa, K.; Nagata, M.; Iida, K.; Dewa, T.; Yamashita, K.; Nango, M. *Colloids Surf. B: Biointerface* **2007**, *56*, 182−187.

BM070352Z